Potential assessment model for Main Hawaiian Islands Yellowfin Tuna Populations

DRAFT

Final Report

John Sibert*
Joint Institute of Marine and Atmospheric Research
University of Hawai'i at Manoa
Honolulu, HI 96822 U.S.A.

April 17, 2015

Introduction

The Yellowfin Tuna (YFT) population in main Hawaiian Islands (MHI) is embedded in a larger pan-Pacific stock. Nevertheless, local fishermen believe that the MHI supports a "resident" yellowfin population which spawns in the MHI. Some scientific observations are consistent with this belief. Recent tagging and tracking studies show that the rate of exchange between the MHI

*sibert@hawaii.edu

population and the larger stock is low (Itano and Holland 2000). Analysis of YFT otoliths sampled from throughout the Pacific conclude that 90% or more of the MHI population was pawned reared in the MHI (Wells et al 2012). The average annual catch of YFT in the MHI from 2008 through 2012 by Hawaii based fleets was approximately 814 mt. Although the MHI fishery is quite small in comparison to the current 550,000 mt WCPO catch (Davies, at al 2014) and is embedded in a much larger stock, management of this fishery is an important local issue deserving of scientific support.

This paper explores potential models that might be used to inform development of options for the management of fisheries for YFT in the MHI.

The principle assumptions for modeling the MHI YFT population are:

1. The Pacific Ocean near Hawaii is divided into two regions: MHI (region 1) and elsewhere (region 2).

2. Fish emigrate from region 1 to region 2, but emigrant fish have no effect on region 2 population dynamics, i.e., region 2 is an "infinite sink".

3. Fish immigrate from region 2 to region 1, and mix completely.

4. Immigrant fish are indistinguishable from "resident" fish (i.e., both groups of fish have the same population dynamics) and interact identically with the fishing gear in region 1.

5. Immigration into the MHI is dependent on the biomass of the yellowfin population outside of the MHI as estimated by some other model, e.g., MULTIFAN-CL (MFCL) or SEAPODYM.

6. The fishery comprises several gear types, each characterized by a distinct fishing mortality.

7. The evolution of fishing mortality over time is a random walk, i.e., the fishing mortality in the current time step is equal to the fishing mortality in the previous time step plus a random deviation.

Data

Several sources of data are used in this analysis:

1. Yellowfin catch weights reported to the Hawaii Department of Aquatic Resources (HDAR) from 1949 to 2014.

2. Longline yellowfin catch weights reported to the National Oceanic and Atmospheric Administration, National Marine Fisheries Service (NOAA) under the federally mandated log book program from 1995 through 2013.

3. Measurements of average yellowfin fish weights sampled at the Honolulu auction by NMFS staff from 2000 through 2013.

4. Model estimates of yellowfin biomass by MFCL from the most recent Western and Central Pacific Fisheries Commission (WCPFC) stock assessment (Davies et al 2014) from 1952 through 2012.

All data are reported by quarter of the year.

Catch Time Series

The HDAR data comprise catch reports for the following gear categories: "Aku boat", "Bottom/inshore HL", "Longline", "Troll", "Tuna HL", "Casting", "Hybrid", "Shortline", "Other", and "Vertical line". For this analysis catches by "Casting", "Hybrid", "Shortline", "Other", and "Vertical line" are combined into a new category, "Misc.". The "Misc" catches are highest after year 2000, but comprise a very small proportion of the catch. The catch time series for the HDAR data are shown in Figure 1. These time series exhibit marked annual cycles suggesting a strong seasonal signal in the catches by all gears. Some series also contain sustained periods of zero catch which document the development and subsequent shift away from a specific gear type. It is assumed that these declines in catches represent a "collapse" of a fishery due more to social and economic factors than to a decline of stock. Some time series are punctuated by brief episodes (one or two quarters in length) of zero catches. Again, it is assumed that these zero catches are not caused by low stock levels.

The longline fishery has changed drastically over time. In the late 1940s, it was a relatively small fishery using traditional tarred rope gear, often labeled "flag line". Participation in this fishery generally declined from 1950 to late 1980s, as can be seen in the time series plots. In the 1990s, the longline fishery expanded rapidly with the introduction of US fishing boats from the Atlantic ocean using modern monofilament longline gear capable of making both deep and shallow sets.

Figure 1 also displays the first order differences between successive quarters. This statistic emphasizes the seasonal periodicity of all fishing gear and helps to identify potential anomalies in the data such as changes in reporting protocols.

The partial autocorrelations within each time series are shown in Figure 2. These correlations confirm the quarterly periodicity of the catch time series. The catch time series for Inshore HL, Longline, Troll, and Tuna HL show similar patters with significant positive autocorrelations at lags of 1,3 and 4 quarters. The autocorrelation pattern appears to be somewhat different for the Aku boat catch time series.

NOAA began to collect data from the longline fleet under a federally mandated logbook program in 1990, and in 1995, began to distinguish deep and shallow sets in the data. The HDAR data do not distinguish between deep and shallow sets. Figure 3 shows the correspondence between the HDAR and NOAA time series. The combined deep plus shallow catches from NOAA line up fairly well with the overlapping HDAR data. The simple average of the HDAR data with the combined NOAA deep plus shallow data appears to have roughly the same autocorrelation structure as the constituent time series, Figure 4. Data are also available from NOAA for the period 1990-1995, but have not yet been included in this analysis.

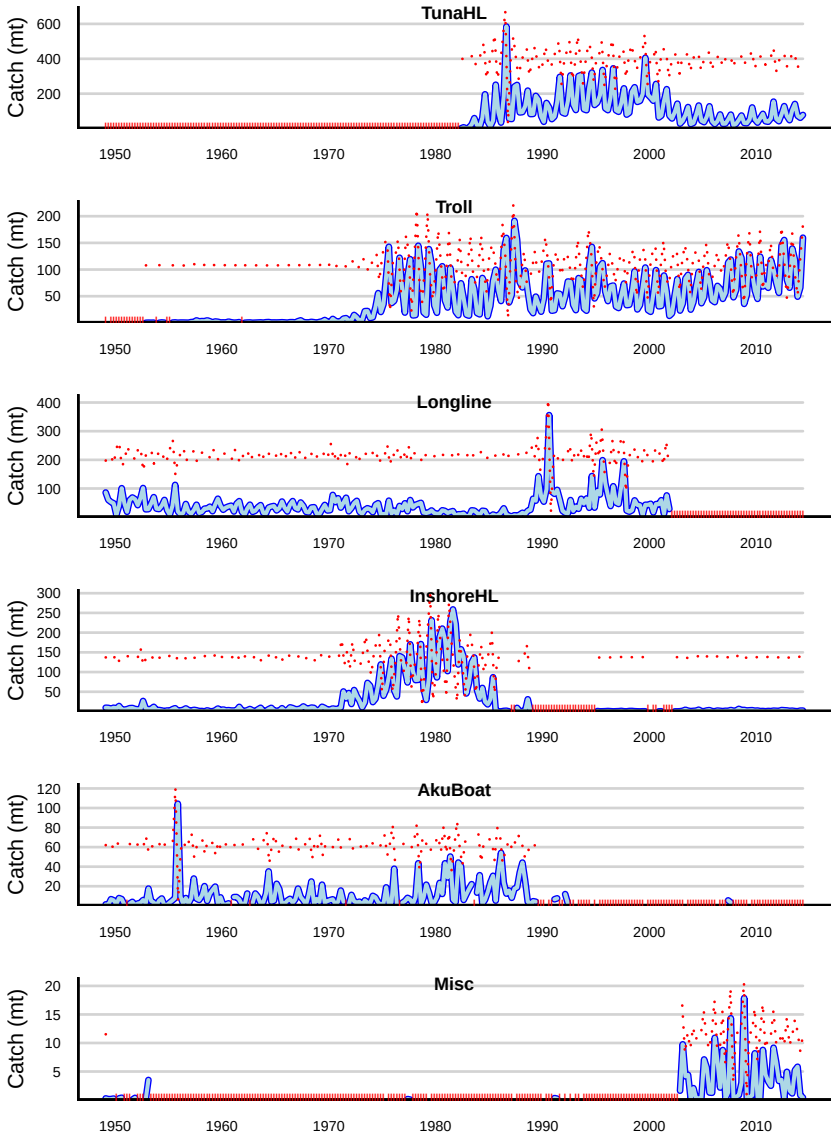

Figure 1: Yellowfin catch in metric tonnes by principle fisheries operating in the Main Hawaiian Islands from the HDAR data. The dotted red line superimposed on each time series is the difference in catch between successive quarters. The red tick marks on the abscissa indicate quarters where catches were zero.

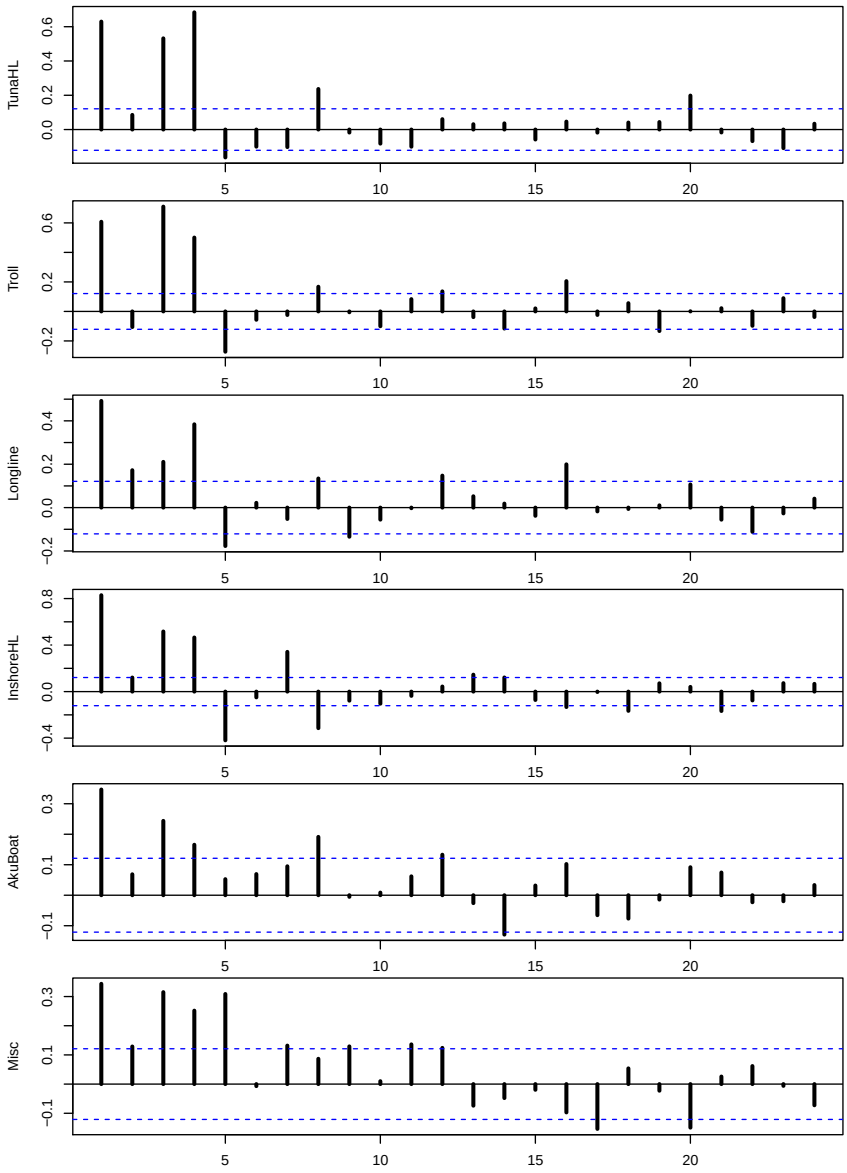

Figure 2: Partial autocorrelation coefficients of the HDAR catch time series. The dashed blue lines indicate approximate 95% confidence limits of the correlations.

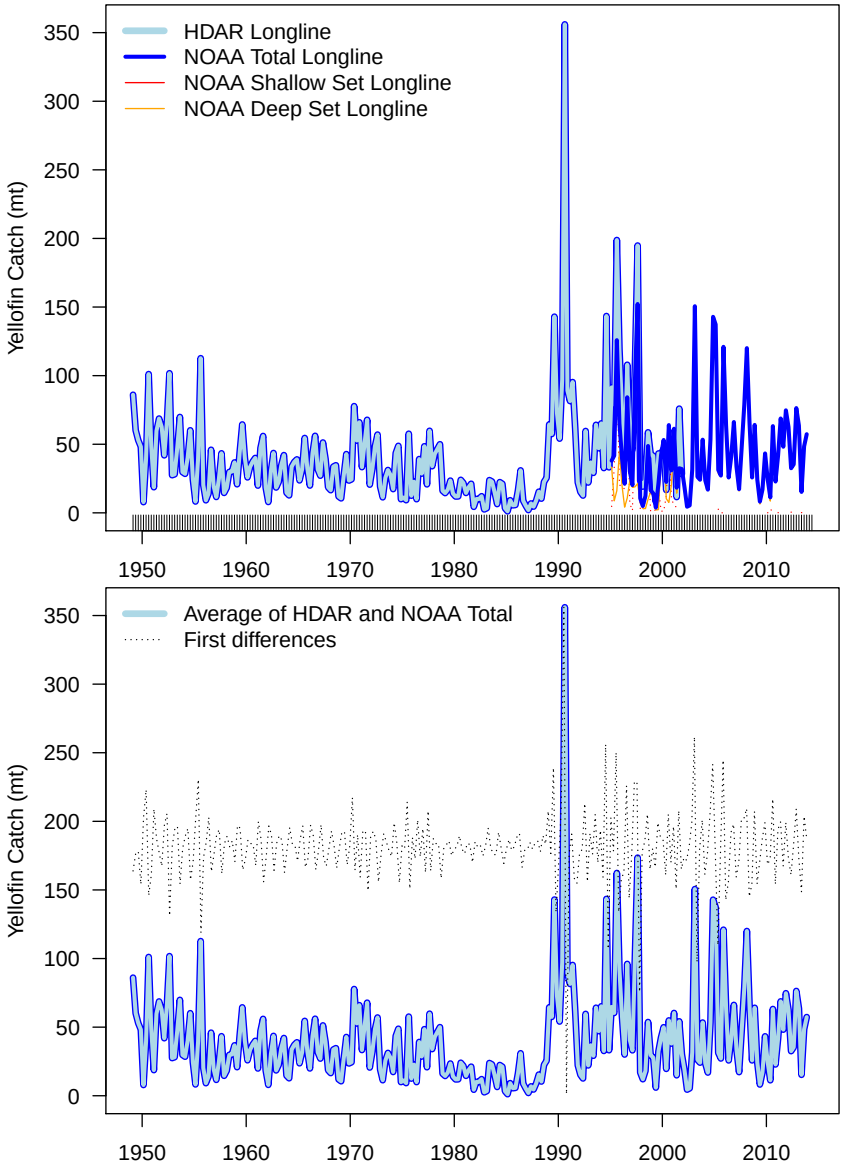

Figure 3: Comparison between HDAR and NOAA longline time series. The upper panel shows the NOAA deep and shallow set data superimposed on the HDAR data. The lower panel shows the time series produced by a simple average of the HDAR data and the sum of the NOAA deep and shallow catches.

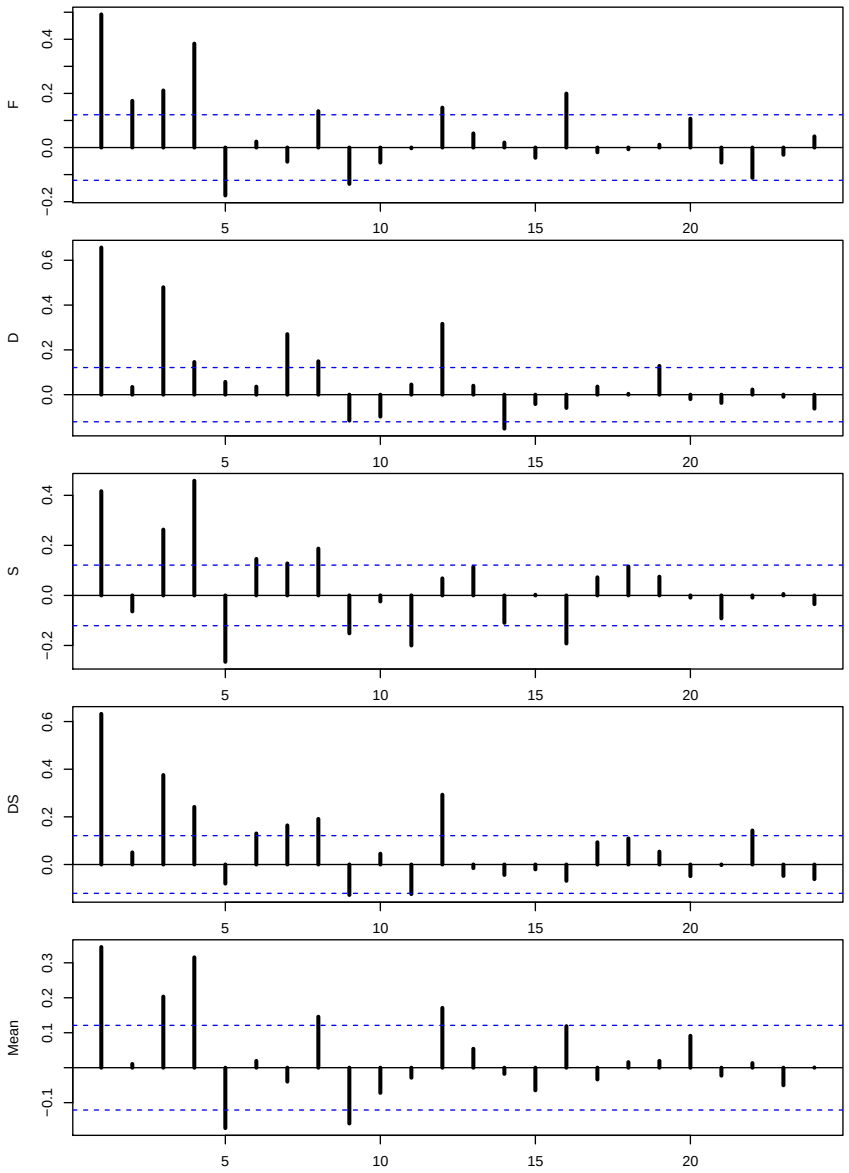

Figure 4: Partial autocorrelations within the NOAA and combined time series. F refers to the HDAR longline data, D refers to the NOAA deep set data, S to the shallow set data, DS to the combined deep and shallow set data, and Mean to the average of the HDAR and NOAA deep plus shallow.

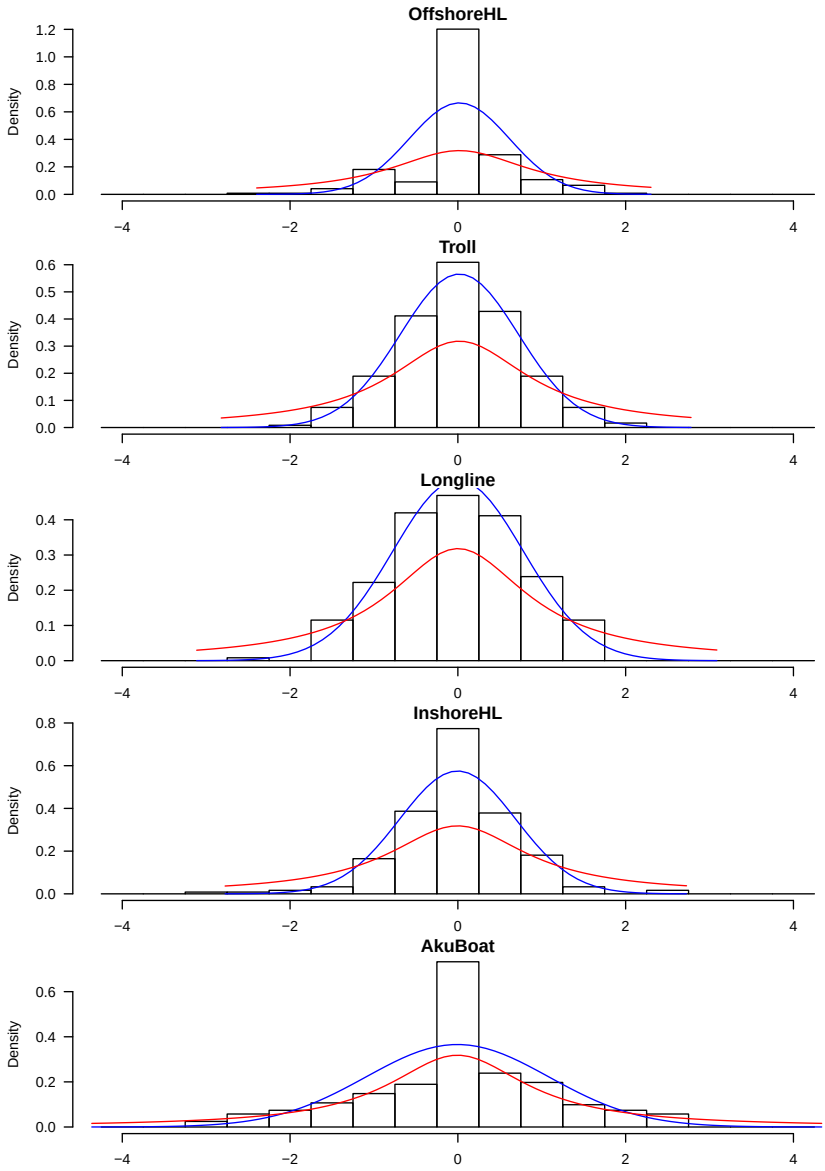

Figure 5: Histograms of first differences of the logarithm of catch time series. The blue line is a normal distribution with the same mean and standard deviation as the first differences. The red line is the equivalent t-distribution.

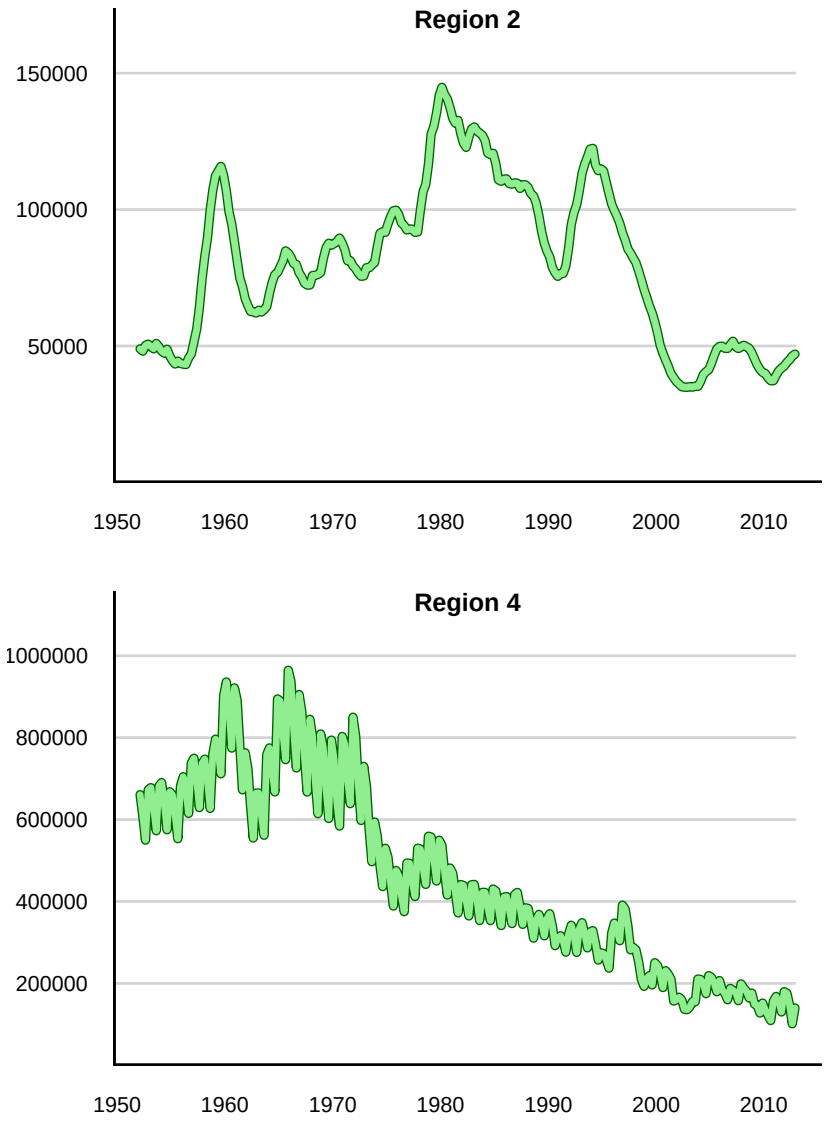

Figure 6: Estimates of biomass in MFCL Regions 2 and 4 from the 2104 WCPFC YFT stock assessment, Davies et al. 2014. The green lines are the biomass trends.

Models

The general modeling approach is to develop a state-space model similar to that utilized by Nielsen and Berg (2014). State-space models separate variability in the biological processes in the system (transition model) from errors in observing features of interest in the system (observation model). The general form of the transition equation is

$$\alpha_t = T(\alpha_{t-1}) + \eta_t \tag{1}$$

where the function T embodies the stock dynamics mediating the development of the state at time t from the state at the previous time with random process error, η. The general form of the observation equation is

$$x_t = O(\alpha_t) + \varepsilon_t \tag{2}$$

where the function O describes the measurement process and with error ε

Age-aggregated model: logistic population dynamics

Let $N_{1,1}$ equal the biomass of fish originating in region 1 and residing in region 1 and $N_{2,1}$ equal the biomass of fish originating in region 2 but residing in region 1. The total biomass of fish residing in region 1 is $N_{1,1} + N_{2,1}$, and the dynamics of the population in region 1 is represented as a modified Schaefer Model:

$$\frac{d}{dt}\big(N_{1,1} + N_{2,1}\big) = \big(N_{1,1} + N_{2,1}\big)\Big[r\Big(1 - \frac{N_{1,1} + N_{2,1}}{K}\Big) - F - T_{12}\Big] + T_{21} \tag{3}$$

where r is the logistic growth rate per quarter, K is the asymptotic biomass, F is the total fishing mortality in region 1, T_{12} is the emigration rate from

region 1 to region 2, and T_{21} is the rate of immigration of biomass from region 2 to region 1.

An equivalent differential equation could be devised for the dynamics of fish residing in region 2 (i.e., $\frac{d}{dt}\big(N_{2,2} + N_{1,2}\big)$), but the dynamics of the fish population in region 2 is external to this model. T_{21} can be considered to be form of population "forcing" by the larger stock in which the MHI population is embedded. T_{21} could be a prediction from other models, such as MULTIFAN-CL or SEAPODYM, in a sort of "off-line" coupling.

The appearance of $N_{1,1} + N_{2,1}$ in the numerator of the logistic term reflects the assumption that the population dynamics of immigrant fish depends on the population dynamics in region 1. This assumption leads to an important non-linearity in the model that predicts of overwhelming of the local stock by a more numerous immigrant stock.

The proportion of "local" fish $p = \frac{N_{1,1}}{N_{1,1}+N_{2,1}}$ is of potential interest. Equation 3 can be expanded and rearranged to become

$$\begin{aligned} \frac{d}{dt}\big(N_{1,1} + N_{2,1}\big) &= N_{1,1}\Big[r\Big(1 - \frac{N_{1,1}}{K}\Big) - F - T_{12}\Big] \\ &+ N_{2,1}\Big[r\Big(1 - \frac{N_{2,1}}{K}\Big) - F - T_{12}\Big] + T_{21} \\ &- 2r\frac{N_{1,1}N_{2,1}}{K} \end{aligned} \tag{4}$$

The non-linear term, $2r\frac{N_{1,1}N_{2,1}}{K}$, in equation 4 represents the reduction in biomass of one population by the presence of the other population. In order to represent the two populations by separate equations, this nonlinear term must be appropriately apportioned. A new parameter, q, is introduced to accomplish the apportionment, leading to a set of simultaneous non-linear

differential equations for the components of the population inhabiting region 1.

$$\begin{aligned}\frac{dN_{1,1}}{dt} &= N_{1,1}\Big[r\Big(1-\frac{N_{1,1}}{K}\Big)-F-T_{12}\Big]-(1-q)2r\frac{N_{1,1}N_{2,1}}{K}\\ \frac{dN_{2,1}}{dt} &= N_{2,1}\Big[r\Big(1-\frac{N_{2,1}}{K}\Big)-F-T_{12}\Big]-q2r\frac{N_{1,1}N_{2,1}}{K}+T_{21}\end{aligned} \tag{5}$$

The log transformed equivalent of equation 5 is

$$\begin{aligned}\frac{d\log(N_{1,1})}{dt} &= r\Big(1-\frac{N_{1,1}}{K}\Big)-F-T_{12}-(1-q)2r\frac{N_{2,1}}{K}\\ \frac{d\log(N_{2,1})}{dt} &= r\Big(1-\frac{N_{2,1}}{K}\Big)-F-T_{12}-q2r\frac{N_{1,1}}{K}+\frac{T_{21}}{N_{2,1}}\end{aligned} \tag{6}$$

Transition Equation $T(\alpha_{t-1})$**.** The state space transition equation for the two components of the MHI population is developed by solving equations 6 by finite differences with explicit time stepping and adding process error terms.

$$\begin{aligned}\log N_{1,1_t} &= \log N_{1,1_{t-\Delta t}}\\ &+ \Delta t\bigg(r\Big(1-\frac{N_{1,1_{t-\Delta t}}}{K}\Big)-\sum_{g=1}^{n}F_{g,t-\Delta t}-T_{12}-(1-q)2r\frac{N_{2,1_{t-\Delta t}}}{K}\bigg)+\eta_{1,t}\end{aligned} \tag{7}$$

$$\begin{aligned}\log N_{2,1_t} &= \log N_{2,1_{t-\Delta t}}\\ &+ \Delta t\bigg(r\Big(1-\frac{N_{2,1_{t-\Delta t}}}{K}\Big)-\sum_{g=1}^{n}F_{g,t-\Delta t}-T_{12}-q2r\frac{N_{1,1_{t-\Delta t}}}{K}+\frac{T_{21_{t-\Delta t}}}{N_{2,1_{t-\Delta t}}}\bigg)+\eta_{2,t}\end{aligned}$$

where $\eta_{k,t}\sim N(0,\Sigma_\eta), k=1,2$. The covariance matrix, $\Sigma_\eta=\begin{bmatrix}\sigma^2_{\eta,1} & \rho_\eta\\ \rho_\eta & \sigma^2_{\eta,2}\end{bmatrix}$,

expresses process errors for both populations as well as a correlation between the errors.

Behavior of model system. Efforts to derive an analytical expression to determine a meaningful equilibrium for equations 6. have not been fruitful. Figure 7 shows phase plane diagrams for several combinations of model parameters assuming constant K and T_{21}. Apparently the system tends towards equilibrium with both $0 < N_{1,1} \leq K$ and $0 < N_{2,1} \leq K$. The proportion of "local" fish, $p = \frac{N_{1,1}}{N_{1,1}+N_{2,1}}$, depends on the assumed value of q. For values of $q < 0.5$, the equilibrium value of p is less than 0.9. The functional relationship, if any, between p and q is not clear, but it would appear that q must be be greater than $\simeq 0.5$ to achieve $p = 0.9$.

The evolution of the model system equation 7 with time is shown in Figure 8. The system starts with $N_{1,1} + N_{2,1} = K$ and $p = 0.9$. After a few time steps the population decreases to reflect competition from the immigrants and the onset of fishing. The total population fluctuates fairly widely, reflecting the forcing from region MFCL 2. The proportion local fluctuates around 0.9.

Fishing Mortality. Fishing mortality is modeled explicitly as a random walk without recourse to effort standardization or estimation of catchability coefficients. The logarithm of fishing mortality is assumed to follow a random walk with normal increments, i.e.,

$$\log F_{g,t} = \log F_{g,t-1} + \xi_{g,t}; \quad \xi_{t,g} \sim N(0, \sigma^2_{\xi,g}) \tag{8}$$

where $\sigma^2_{\xi,g}$ is the variance of the fishing mortality random walk for gear g, $g =$

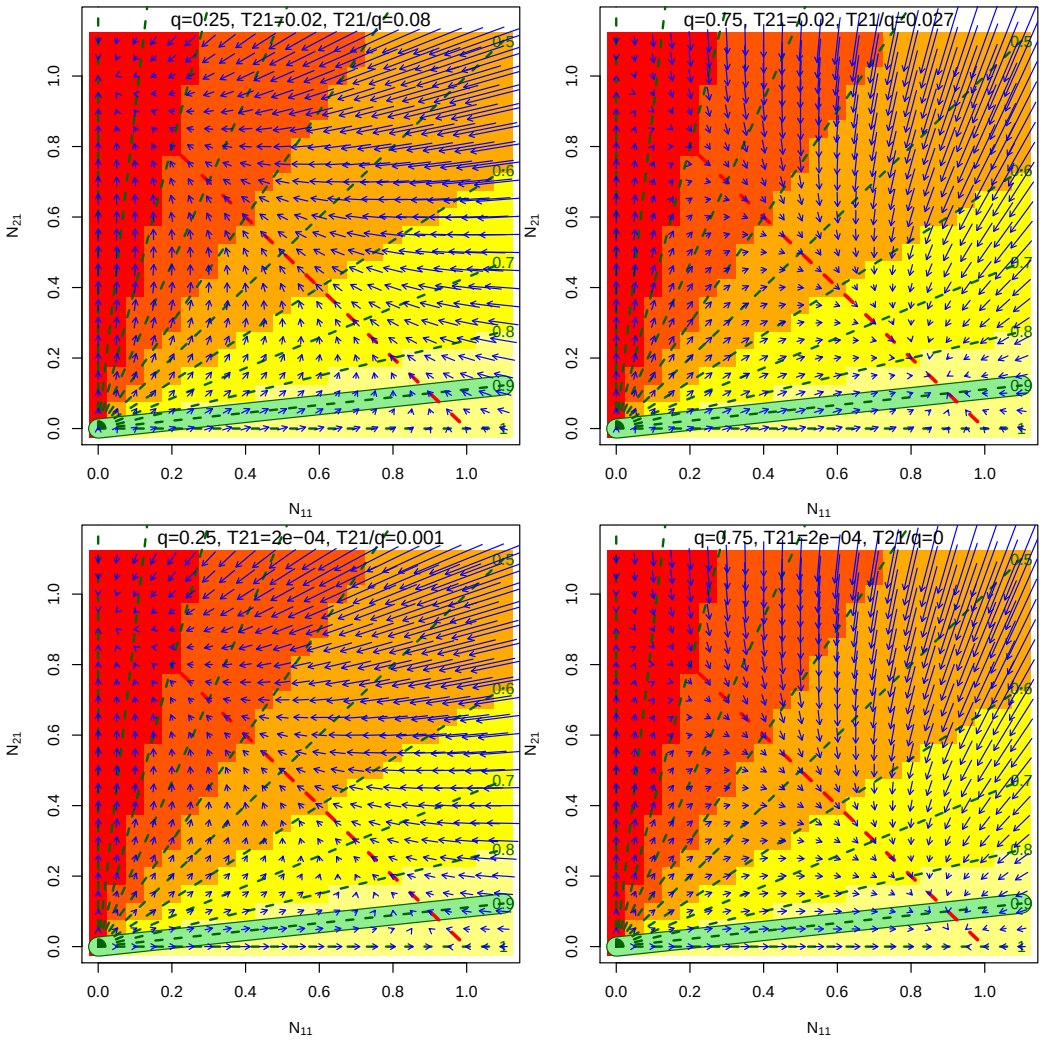

Figure 7: Phase plane for equation 6. Arrows represent the trajectory of the system for different combinations of $N_{1,1}$ and $N_{2,1}$; dashed red line indicates $K = 1$; dashed green lines indicate different values of p. The thick light green line indicates $p = 0.9$. Values of q and T_{21} are shown in each panel. Other parameter values: $r = 0.3, K = 1.0, F = 0.007, T_{12} = 0.01$.

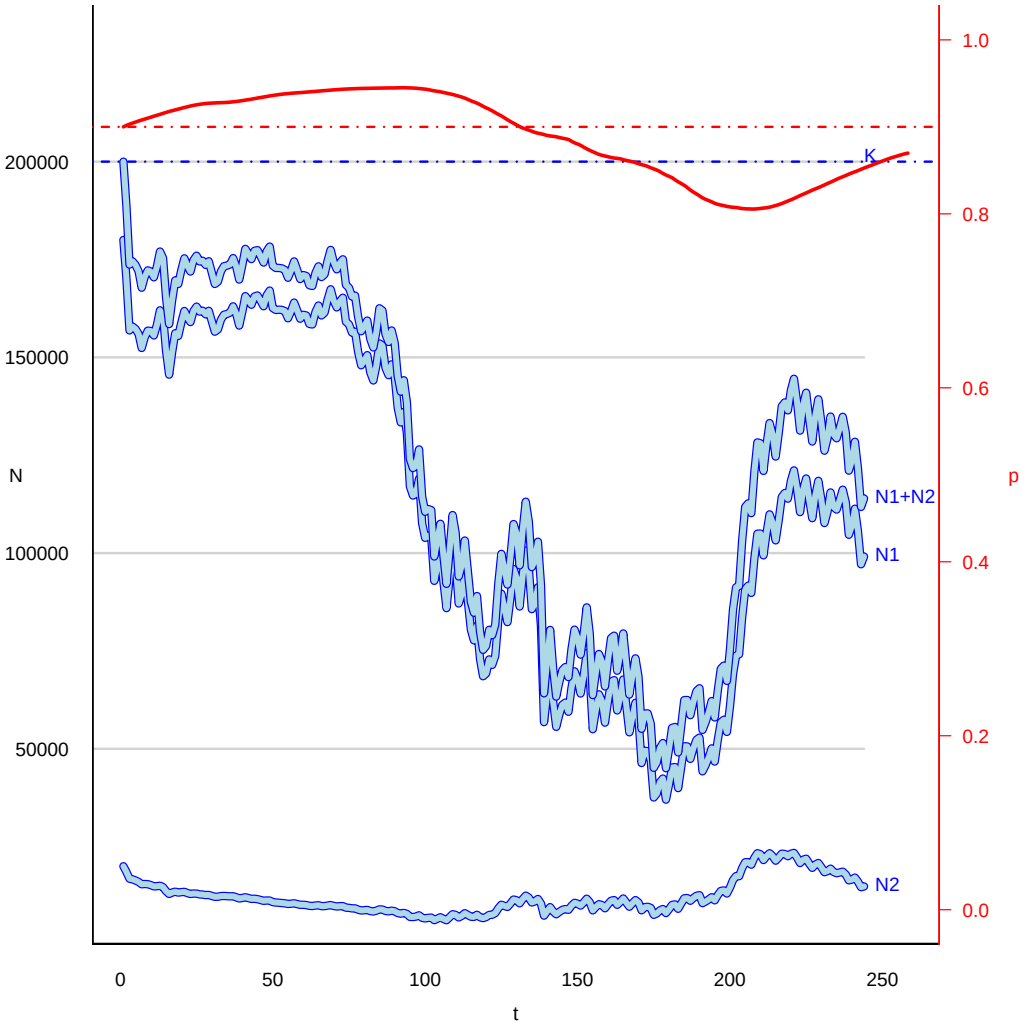

Figure 8: Behavior of equations 7 over time with forcing from MFCL region 2 biomass (Figure 6) and fishing mortality by fleet set proportional to observed catch. Light blue lines indicate population components as indicated; dashed blue line indicates K; solid red line indicates the proportion local, p; dashed red line line indicates $p = 0.9$. Other parameter values: $q = 0.54, r = 0.3, K = 200000, T12 = 0.01, T21 = 0.002$.

$1 \ldots n$.

Population Forcing. Immigration of stock from region 2 to region 1 is a form of forcing whereby events outside of the model influence the model dynamics. The term T_{21_t} in equation 7 is the biomass immigrating into the MHI stock at each time step. The likely candidates for forcing are MFCL regions 2 and 4, both of which overlap the MHI. The estimated biomass trajectories for these two regions are shown in Figure 6. For testing purposes, I assume that the source of immigrants is MFCL region 2, so that

$$T_{21_t} = T^*_{21} \cdot B_{2,t} \tag{9}$$

where $B_{2,t}$ is biomass in region 2 at time t taken from the MFCL output file `plot-12.par.rep` from the 2014 WCPFC stock assessment (Davies et al 2014). T^*_{21} is the proportion on $B_{2,t}$ which migrates at each time step. Alternatively, $B_{2,t}$ may be assumed to be constant at the average of the estimated biomass in region 2, $\overline{B_2}$.

Asymptotic biomass. K is the asymptotic biomass in a population growing according to logistic dynamics. It is the population size to which the population tends at equilibrium and is often dubbed "carrying capacity". It is not clear that a coupled logistic model such as equation 3 has a non-trivial equilibrium. Furthermore, the $B_{2,t}$ is time dependent, Figure 6. Several alternative parameterizations of K can be envisaged, for example, constant at the maximum of $B_{2,t}$, an unknown parameter, or even a random walk. For testing purposes I have assumed the maximum of $B_{2,t}$ because the maximum biomass is lower in region 2 and appears less depleted than in region 4.

Given that the model forcing $B_{r,t}$ is not constant and that the fishery is developing in a period of profound change in the oceans, it is difficult to justify the assumption that the equilibrium population size, K, has been constant for over 50 years. An alternative parameterization for K is to assume a random walk, for example,

$$\log K_t = \log K_{t-1} + \omega_t; \quad \omega_t \sim N(0, \sigma_\omega^2) \tag{10}$$

where σ_ω^2 is the variance of the asymptotic population size random walk. This parameterization was implemented in code, but not extensively tested.

Observation Equation, $O(\alpha)$. Predicted catch in region 1 is the product of fishing mortality and the total population in region, $N_{1,1} + N_{2,1}$. Thus the state-space observation model predicting catch in the region 1 under this model is

$$\log C_{g,t} = \log\left(F_{g,t} \cdot \left(\frac{{N_{1,1}}_{t-\Delta t} + {N_{1,1}}_t}{2} + \frac{{N_{2,1}}_{t-\Delta t} + {N_{2,1}}_t}{2}\right)\right) + \varepsilon_{t,g} \tag{11}$$

where the total population in region 1 is the sum of the average population over the time step (Quinn and Deriso, 1999), and $\varepsilon_{t,g} \sim N(0, \sigma_{\varepsilon,g}^2)$.

Constraint on "Proportion Local". Proportion local is defined as $p = \frac{N_{1,1}}{N_{1,1}+N_{2,1}}$. The logit transformed proportion local, $L(p)$, is assumed to be normally distributed around a mean value, $L(\bar{p})$.

$$L(p) \sim N(L(\bar{p}), \sigma_{L(p)}^2). \tag{12}$$

p is generally assumed to be approximately 0.9. By varying the value of the variance, $\sigma_{L(p)}^2$, p can be made as close to 0.9 as is prudent. This representation of p can be interpreted as a Bayesian prior. In principle, it may be

possible to estimate $\bar{p}$ and $\sigma^2_{L(p)}$, but interactions with the parameter q in equation 5 should be explored.

Estimation. The model states, α_t, are assumed to be random effects (Skaug and Fournier, 2006). Model parameters are estimated by maximizing the joint likelihood of the random effects and the observations.

$$L(\theta, \alpha, x) = \prod_{t=2}^{m} \left[\phi\big(\alpha_t - T(\alpha_{t-1}), \Sigma_\eta\big)\right] \prod_{t=1}^{m} \left[\phi\big(x_t - O(\alpha_t), \Sigma_\varepsilon\big)\right] \tag{13}$$

Here, m is the number of time steps in the catch time series and θ is a vector of model parameters. A complete list of parameters is found in Table 1. The model is implemented in AD Model Builder (Fournier et al 2012). The actual number of parameters to be estimated depends on the model configuration, specified by phase flags in the input file. All computer code, data files, and draft reports in support of this analysis can be found at Github: `https://github.com/johnrsibert/XSSA.git`.

Results & Discussion

Initial model testing gives mixed results. The numerical estimation procedure inevitably terminates with the dreaded error message ‘‘`Matrix not positive definite in Ln_det_choleski`’’. Values of the model parameters just prior to termination of the program are compared to their initial values in Table 2. The model seems sensitive to the population dynamics parameters. The values of the growth rate and transfer rates parameters (r, T_{12}, T^*_{21}) change substantially from their initial values. The state equation process errors, $\sigma_{1,\eta}, \sigma_{2,\eta}$, also move away from their initial values. The pro-

Table 1: Model variables.

Variable	Definition
m	Number of quarterly time steps
n	Number of fishing gears
r	Instantaneous growth rate (q^{-1})
K	Asymptotic biomass (mt)
T_{12}	Emigration rate (q^{-1})
T_{21}^{*}	Immigration rate (q^{-1})
$\sigma_{1,\eta}, \sigma_{2,\eta}$	Population growth SD
ρ_{η}	Correlation between population growth precess errors
$\sigma_{\xi,g}\ g = 1 \ldots n$	Fishing mortality random walk SD
$\sigma_{\varepsilon,g}\ g = 1 \ldots n$	Observation error SD
$\bar{p}$	Mean proportion local
$\sigma_{L(p)}$	SD logit transformed p
q	Nonlinear apportionment proportion
$a_g\ g = 1 \ldots n$	Proportion of F random walk contaminated by fat-tailed distribution

cess error correlation, ρ, is not yet implemented in the model code which is equivalent to constraining ρ to be zero.

The random-walk representation of fishing mortality produces a credible time series capable of accurately predicting catches of all 5 gear types in the model, Figures 9 and 10. These estimates of F depend on a "robust" likelihood representation of the variance of the random walk with a 5% contamination by a fat-tailed distribution to accommodate outliers; a_g in Table 2.

Fifteen parameters are used to represent the variance in catch, a_g, $\sigma_{\varepsilon,g}$ and $\sigma_{\xi,g}$. These parameters are changed little or not at all by the estimation procedure, suggesting that some are redundant. It may be possible to represent these errors by a single parameter for each fleet.

The predicted biomass corresponding from the test run is shown in Figure 11. After some fluctuations at the beginning of the time series the total biomass, $N_{1,1} + N_{2,1}$, appears to stabilize to a constant value slightly below the asymptotic biomass, K. The proportion local stays close to 0.9 as it is constrained to do by the prior, equation 12. In other test runs (not illustrated here), the total biomass is less steady and has an increasing and subsequent decreasing trend reflecting the trend in the forcing biomass. The cause of the initial fluctuation in Figure 11 is unknown. The procedure seems to set the initial population random effects higher than K for some reason.

The catch time series include a fairly large number of zero catch observations, Figures 1 and 5. Zero observations at the beginning of the time series, as the fishery develops, or at the end of the time series, as a particular fleet

ceases operation, do not appear to cause problems in estimating F. However, in the case of the Troll, Inshore Handline and Aku Boat fleets, there are isolated quarters where the reported catch is zero during periods of substantial catch. In early test runs of the model, these observations caused the model to predict zero biomass at those quarters followed by periods of recovery. The problem of intercalated zero observations was provisionally solved by substituting the average of the immediately preceding and following observations for the intercalated zero observation. There are 9 such substitutions among the 1220 observations. Another approach would be to shift annual time steps, thus averaging out the zero observations.

There appear to be excessive numbers of zero first differences in the data for most gears, Figure 5. Only one gear, Aku Boat, appears to have particularly fat tails. A zero inflated distribution may be a better choice of error model for the fishing mortality random walk than a robustified Normal.

Model feasibility and Next steps

The age-aggregated approach using a logistic model with emigration and immigration appears to be feasible and shows sufficient promise to continue model development. The general behavior of the model system (Figures 7 and 8) appropriately describes a small persistent population interacting with a much larger one. The efficacy of the random walk representation of fishing mortality is particularly encouraging, and avoids debates about changes in catchability associated with changes in fishing efficiency. The propor-

Table 2: Model "estimates". Initial values of model parameters and final values just prior to program exit with "Matrix not positive definite in Ln_det_choleski" message. "—" indicates that the variable was constrained to be constant at its initial value, i.e., not estimated.

Vatiable	Initial Value	Final Value
m	244	
n	5	
r	0.100	0.292
K	144,800	—
T_{12}	0.018	0.0116
T^*_{21}	0.018	0.00171
$\sigma_{1,\eta}$	0.378	0.120
$\sigma_{2,\eta}$	0.378	0.216
ρ_η	0.0	—
$\sigma_{\xi,1}$	0.368	0.368
$\sigma_{\xi,2}$	0.368	0.368
$\sigma_{\xi,3}$	0.368	0.368
$\sigma_{\xi,4}$	0.368	0.368
$\sigma_{\xi,5}$	0.368	0.368
$\sigma_{\varepsilon,1}$	1.051	1.042
$\sigma_{\varepsilon,2}$	1.051	1.045
$\sigma_{\varepsilon,3}$	1.051	1.045
$\sigma_{\varepsilon,4}$	1.051	1.045
$\sigma_{\varepsilon,5}$	1.051	1.050
$\bar{p}$	0.9	—
$\sigma_{L(p)}$	2.72	—
q	0.54	—
a_1	0.05	—
a_2	0.05	—
a_3	0.05	—
a_4	0.05	—
a_5	0.05	—

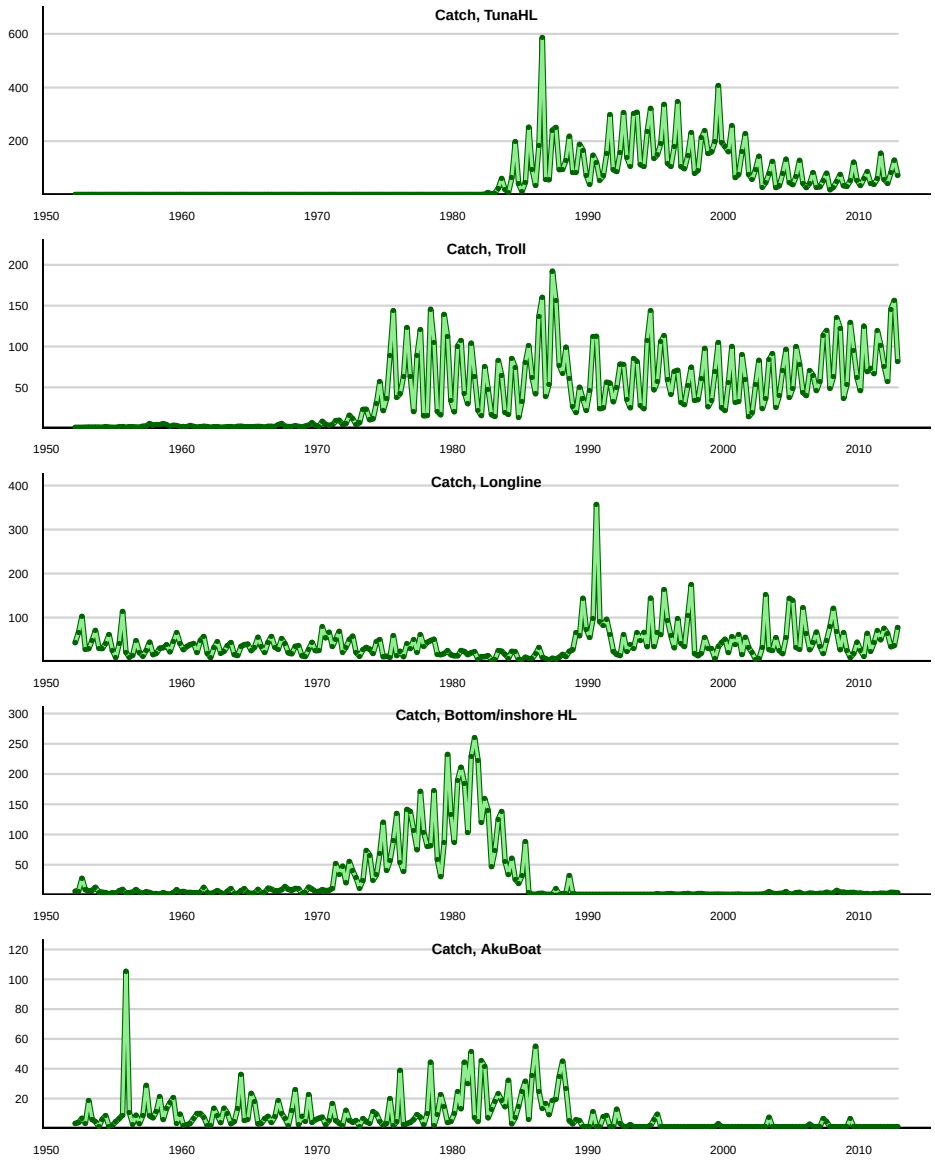

Figure 9: Estimated catch by fleet in metric tons. The dark green dots indicate observed catch and light green lines indicate predicted catch,

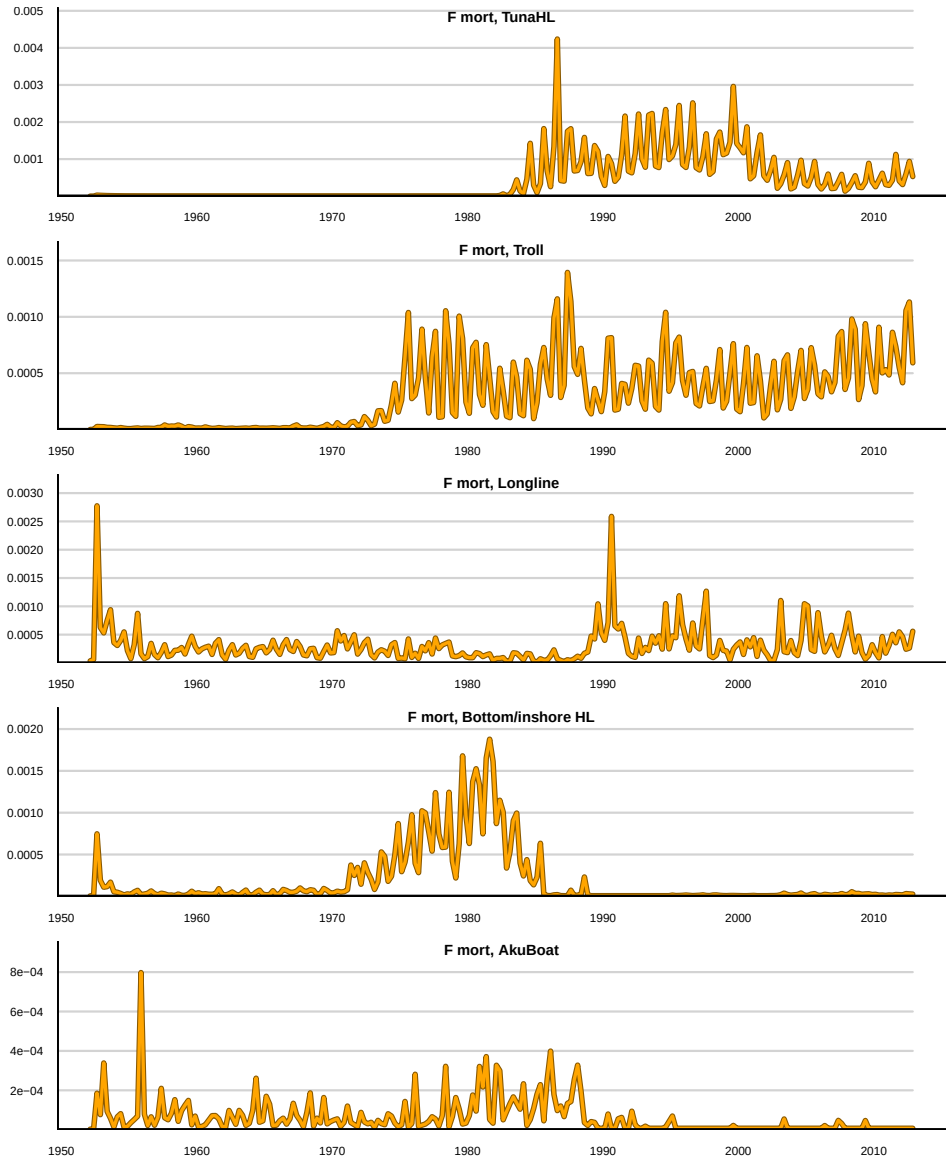

Figure 10: Estimated fishing mortality (per quarter) by fleet.

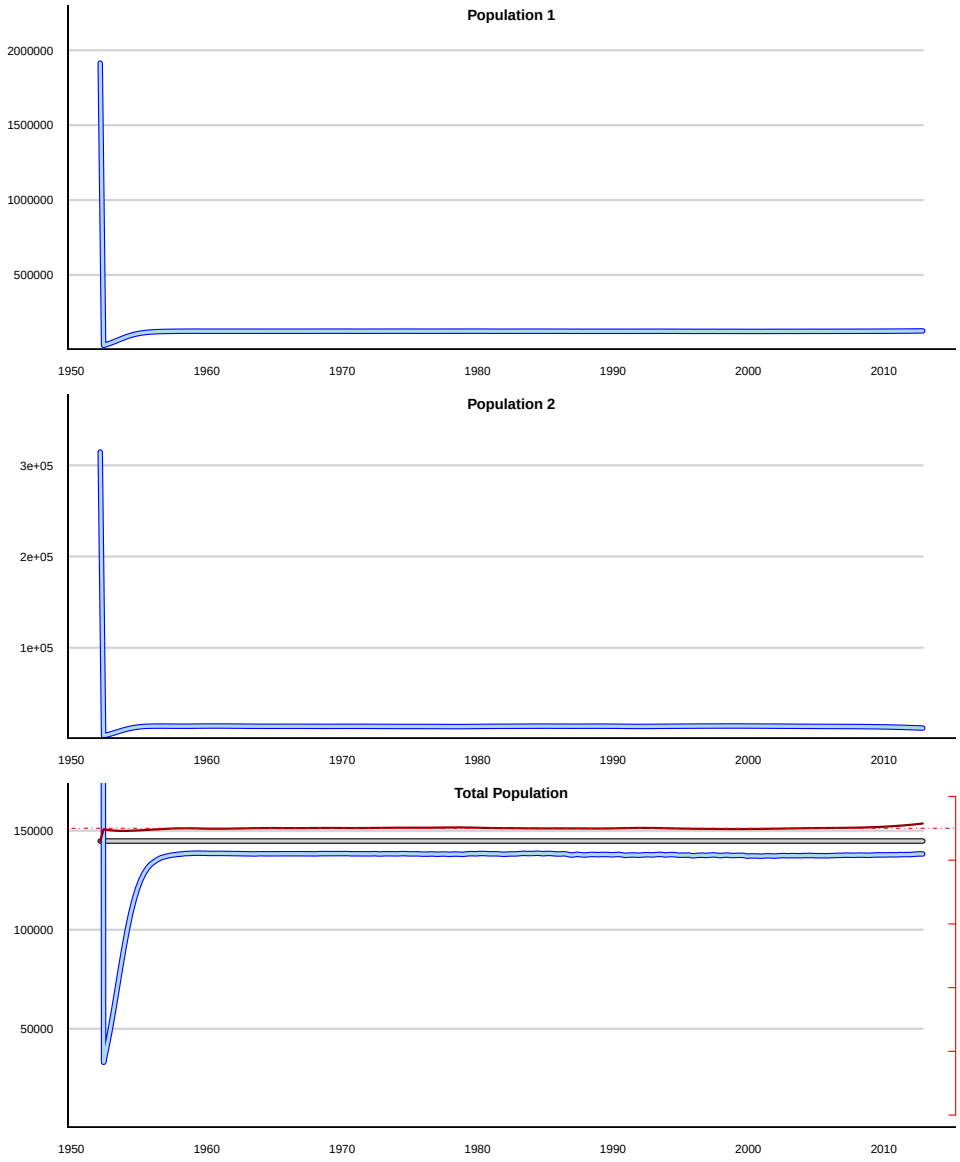

Figure 11: Estimated biomass in metric tons. Light blue lines indicate predicted $N_{1,1}$ (upper panel), $N_{2,1}$ (middle panel) and $N_{1,1} + N_{2,1}$ bottom panel. Red line in bottom panel indicates proportion local; dashed red line indicates $p = 0.9$. Grey line in bottom panel is K.

tion of local fish in the system is sensitive to model parameters and can be constrained to be near the empirically determined value of 0.9. Population growth parameters (including q), exchange rates, and transition model errors all appear to be estimatable. Other variance parameters are not well determined and are in need of refinement.

Some obvious next steps are: use annual catch totals by gear rather than quarterly reports to avoid intercalated zero catches; develop a zero-inflated likelihood to apply either the fishing mortality random walk or the observation error; improve the simulation to enable simulation/estimating testing.

Very little work was directed to development of an age-structured model. Preliminary examination of the weight-frequency data indicate that there is a clear growth signal, but the time series only covers the most recent 13 years. Furthermore, there may be no means to associate the size data with a particular fishing gear. Finally, it is not clear that the weight sampling captures the complete range of active fisheries for yellowfin.

Acknowledgements. This work was funded by the Western Pacific Regional Fisheries Managment Council. I thank the Council for its generous support and Council Staff Paul Dalzell and Eric Kingma for encouraging me to actually take on this challenging project and for their on-going collaboration. Thanks to Mr. David Itano for sharing insights into the small-boat fisheries in Hawaii. Martha Maciasz, student intern at the Council, assisted with processing weight frequency data. Thanks to Mr. Reginald Kokubun of the Hawaii Division of Aquatic Resources for supplying catch report data from the HDAR commercial fisheries data base. Thanks to Mr. Keith Bigelow and Ms. Karen Sender of NOAA Pacific Island Fisheries Science Center for supplying logbook reporting data and weight-frequency data from the PIFSC data base. Thanks also to Dr. John Hampton of the Secretariat of the Pacific Community, Oceanic Fisheries Programme, for making available MULTICAN-CL output files from the latest Western and Central Pacific Fisheries Commission yellowfin tuna stock assessment, and to Mr. Nick Davies for sharing R scripts and advice to decode the MFCL output files.

References

Davies, N., S. Harley, J. Hampton, S. McKechnie. 2014. Stock assessment of yellowfin tuna in the western and central pacific ocean. WCPFC-SC10-2014/SA-WP-04.

Fournier, D. A., H.J. Skaug, J. Ancheta, J.Sibert, J. Ianelli, A. Magnusson, M. N. Maunder, A. Nielsen. 2012. AD Model Builder: using automatic differen-

tiation for forstatistical inference of highly parameterized complex nonlinear models. Opti-mization Methods and Software 27, 233249.

Itano, D., K. Holland. 2000. Movement and vulnerability of bigeye (Thunnus obesus) and yellowfin tuna (Thunnus albacares) in relation to FADs and natural aggregation points.Aquat. Living Resour. 13: 213-223.

Kleiber, P., J. Hampton, N. Davies, S. Hoyle, D. Fournier. 2014. MULTIFAN-CL Users Guide

Nielsen, A., C. Berg. 2014. Estimation of time-varying selectivity in stock assessments using state-space models. Fisheries Research 158:96-101.

Quinn, T, R. Deriso. 1999. Quantitative fish dynamics. Oxford University Press, New York.

Skaug, H., Fournier, D., 2006. Automatic approximation of the marginal likelihood in non-Gaussian hierarchical models. Computational Statistics & Data Analysis 51, 699709.

Wells, D., J. Rooker, D. Itano. 2012. Nursery origin of yellowfin tuna in the Hawaiian Islands. Mar. Ecol. Prog. Ser. 461:187-196.